NASA TECHNICAL MEMORANDUM

NASA TM X-1508

NASA TM X-1508

GPO PRICE $ ______

CSFTI PRICE(S) $ ______

Hard copy (HC) 3.00

Microfiche (MF) .65

ff 653 July 65

FACILITY FORM 602

(ACCESSION NUMBER)	(THRU) 1
15 (PAGES)	(CODE)
(NASA CR OR TMX OR AD NUMBER)	(CATEGORY)

LINE-OF-SIGHT VELOCITY AS AN INDICATOR OF PERICYNTHION ALTITUDE OF SELENOCENTRIC ORBITS

by James Lloyd Williams

Langley Research Center
Langley Station, Hampton, Va.

NATIONAL AERONAUTICS AND SPACE ADMINISTRATION • WASHINGTON, D. C. • MARCH 1968

NASA TM X-1508

LINE-OF-SIGHT VELOCITY AS AN INDICATOR OF PERICYNTHION ALTITUDE OF SELENOCENTRIC ORBITS

By James Lloyd Williams

Langley Research Center
Langley Station, Hampton, Va.

NATIONAL AERONAUTICS AND SPACE ADMINISTRATION

For sale by the Clearinghouse for Federal Scientific and Technical Information
Springfield, Virginia 22151 – CFSTI price $3.00

LINE-OF-SIGHT VELOCITY AS AN INDICATOR OF PERICYNTHION ALTITUDE OF SELENOCENTRIC ORBITS

By James Lloyd Williams
Langley Research Center

SUMMARY

An investigation was made to determine the feasibility of using simplified equations to predict the pericynthion of a selenocentric orbit. It was assumed that the angular rate of the line of sight with respect to a prominent lunar surface feature was available for positions along a ballistic trajectory. The equations used were derived in terms of this variable by utilizing the linearized rendezvous equations and certain parameters of a circular selenocentric orbit. The procedure used in the evaluation of these equations was to calculate the pericynthion of selected reference Hohmann trajectories and to compare the values calculated by these equations with the known reference orbit values.

The results of the computations indicate that

(1) The pericynthion altitude predicted by the approximate equations generally is not accurate.

(2) The predicted pericynthion altitude is very sensitive to the reference orbit altitude, to the times at which measurements of the rotation of the line of sight are made, and to the length of time between the measurements of the angular rate of line of sight.

INTRODUCTION

A critical phase of the lunar mission is the establishment of a safe elliptical transfer orbit between the selenocentric circular orbit of the command module and a prescribed position close to the lunar surface, the pericynthion of the transfer orbit. The final touchdown maneuver is initiated from the pericynthion of the transfer orbit. Moderate errors in the transfer maneuver could result in an unsafe orbit (impact or near impact trajectory) in this phase of the lunar mission. It is apparent that mission reliability could be enhanced if simplified methods of determining orbit pericynthion were available in the event of automatic guidance failure.

Several approaches to simplifying orbit determination, with varying degrees of complexity, have been reported in references 1 and 2. In reference 1 equations based on various combinations of orbital parameters are presented, and in reference 2 errors in pericynthion based on altitude-deviation measurements are evaluated. The approach studied in this investigation made use of the line-of-sight rotational velocity in respect to a prominent lunar surface feature for the determination of orbit pericynthion.

This report presents linearized equations for pericynthion prediction which were derived in terms of the line-of-sight rotational velocity, relative to lunar surface features, by making use of linearized rendezvous equations. Pericynthion altitudes calculated from these equations for three known selenocentric elliptic orbits are also presented. The trajectories selected for these calculations had pericynthions of -186, 10 862, and 27 611 meters.

SYMBOLS

h altitude above lunar surface, meters

Δh_p numerical difference between true pericynthion and predicted pericynthion, meters

m mass of body

r radial distance from center of lunar sphere to vehicle, meters

$\dot{r}$ radial velocity component of vehicle, meters/second

r_m radius of lunar sphere, meters

$r\dot{\theta}$ velocity component of vehicle perpendicular to radius vector, meters/second

t time measured from apocynthion, seconds

x_s relative displacement measured along circular selenocentric orbit from origin of moving axis, meters

y_s relative displacement measured along radius r from end of x_s displacement to landing vehicle, meters

x relative rectangular displacement perpendicular to radius r_o and measured from origin of moving-axis system, meters

y relative rectangular displacement measured along radius r_o from origin of moving-axis system, meters

X,Y,Z moving rectangular coordinate system

θ angular position of vehicle measured from reference position, degree or radian

λ angular separation of moving-axis-system origin and vehicle in orbit

ρ distance from landing vehicle to prominent lunar surface feature, meters

ω angular rate of moving-axis origin in selenocentric orbit, radian/second

ω_{ls} angular rate of line of sight, radians/second

ϕ angle between vehicle's local vertical and line of sight to surface feature, degrees

Subscripts:

p pericynthion

1,2,3 order of reading

o selenocentric circular orbit conditions

Dots over symbols denote derivatives with respect to time.

ANALYSIS

It is desired to ascertain whether orbital characteristics can be obtained from the angular rate of the line of sight with respect to a prominent lunar surface feature. The primary coordinate system used in the derivation of the equations was a cylindrical shell coordinate system the origin of which was assumed to be in a circular selenocentric orbit. A sketch of this system denoted by the displacement components x_s,y_s can be seen in figure 1, along with a typical moving rectangular coordinate system X,Y. A set of transformation equations that connects the shell and rectangular coordinate systems is

$$x = \left(r_o + y_s\right)\sin\left(\frac{x_s}{r_o}\right) \tag{1}$$

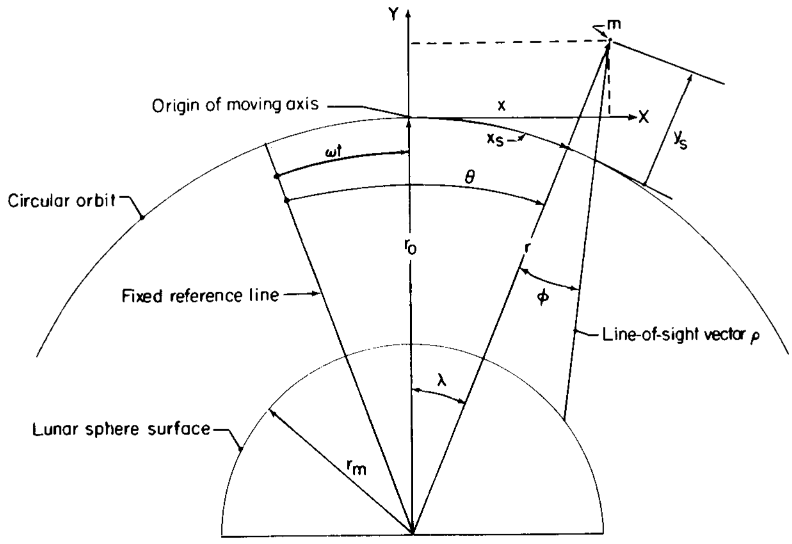

Figure 1.- Sketch of coordinate axis systems, angles, and displacements.

$$y = \left(r_o + y_s\right)\cos\left(\frac{x_s}{r_o}\right) - r_o \tag{2}$$

A typical representation of the geometrical relationships between the line-of-sight and velocity components is shown in figure 2. The vehicle velocity normal to the line of sight can be expressed as follows:

$$\omega_{ls}\rho = (r\dot{\theta})\cos\phi + \dot{r}\sin\phi \tag{3}$$

The velocity components, in polar form, can be expressed as

$$(r\dot{\theta}) = \dot{x}\cos\lambda - \dot{y}\sin\lambda + r_o\omega\cos\lambda$$

$$\dot{r} = \dot{x}\sin\lambda + \dot{y}\cos\lambda + r_o\omega\sin\lambda$$

Equation (3) therefore can be written as

$$\omega_{ls}\rho = \left(\dot{x}\cos\lambda - \dot{y}\sin\lambda + r_o\omega\cos\lambda\right)\cos\phi + \left(\dot{x}\sin\lambda + \dot{y}\cos\lambda + r_o\omega\sin\lambda\right)\sin\phi \tag{4}$$

Differentiation of equations (1) and (2) yields

$$\dot{x} = \dot{y}_s\sin\frac{x_s}{r_o} + \left(r_o + y_s\right)\left(\cos\frac{x_s}{r_o}\right)\frac{\dot{x}_s}{r_o}$$

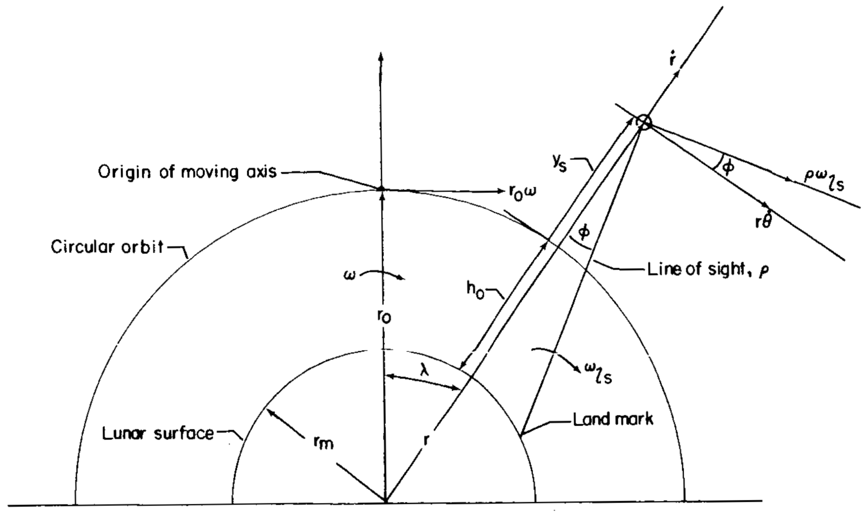

Figure 2.- Sketch showing angular displacements and angular and linear rates.

$$\dot{y} = \dot{y}_s \cos\frac{x_s}{r_o} - \left(r_o + y_s\right)\left(\sin\frac{x_s}{r_o}\right)\frac{\dot{x}_s}{r_o}$$

Use of these relations in equation (4) results in

$$\begin{aligned}
\omega_{ls}\rho = &\left[\dot{y}_s \sin\frac{x_s}{r_o} + \left(r_o + y_s\right)\left(\cos\frac{x_s}{r_o}\right)\frac{\dot{x}_s}{r_o}\right] \cos\lambda \cos\phi \\
&- \left[\dot{y}_s \cos\frac{x_s}{r_o} - \left(r_o + y_s\right)\left(\sin\frac{x_s}{r_o}\right)\frac{\dot{x}_s}{r_o}\right] \sin\lambda \cos\phi \\
&+ r_o\omega(\cos\lambda \cos\phi + \sin\lambda \sin\phi) + \left[\dot{y}_s \cos\frac{x_s}{r_o} - \left(r_o + y_s\right)\left(\sin\frac{x_s}{r_o}\right)\frac{\dot{x}_s}{r_o}\right] \cos\lambda \sin\phi \\
&+ \left[\dot{y}_s \sin\frac{x_s}{r_o} + \left(r_o + y_s\right)\left(\cos\frac{x_s}{r_o}\right)\frac{\dot{x}_s}{r_o}\right] \sin\lambda \sin\phi
\end{aligned} \tag{5}$$

Use of the relation $\lambda = \frac{x_s}{r_o}$ in equation (5) results in

$$\omega_{ls}\rho = \dot{y}_s \sin\phi + \left(r_o + y_s\right)\frac{\dot{x}_s}{r_o} \cos\phi + r_o\omega\left(\cos\lambda \cos\phi + \sin\lambda \sin\phi\right) \tag{6}$$

It is assumed that ϕ and λ are small angles so that $\sin\phi = \phi$, $\cos\phi = 1$; $\sin\lambda = \lambda$, $\cos\lambda = 1$. For this investigation the maximum separation between the origin of the moving axis and the landing vehicle λ was about 6^o. This assumption implies that $\rho \approx h_o + y_s$. Under these assumptions, equation (6) becomes

$$\omega_{ls}\left(h_o + y_s\right) = \dot{y}_s\phi + \left(r_o + y_s\right)\frac{\dot{x}_s}{r_o} + r_o\omega\left(1 + \lambda\phi\right) \tag{7}$$

If it is assumed that $r_o + y_s \approx r_o$ and second-order terms are neglected, equation (7) becomes

$$\omega_{ls}\left(h_o + y_s\right) = \dot{x}_s + r_o\omega \tag{8}$$

Based on linearized equations of motion similar to the method developed in reference 3, the position and velocity of a mass in a nonthrusting trajectory relative to a moving-axis system in a circular orbit are given by the following equations:

$$x_s(t) = \left(\frac{4\dot{x}_s(0)}{\omega} + 6y_s(0)\right)\sin\omega t + \frac{2\dot{y}_s(0)}{\omega}\cos\omega t - \left(6y_s(0) + \frac{3\dot{x}_s(0)}{\omega}\right)\omega t + x_s(0) - \frac{2\dot{y}_s(0)}{\omega} \tag{9a}$$

$$\frac{\dot{x}_s(t)}{\omega} = \left(\frac{4\dot{x}_s(0)}{\omega} + 6y_s(0)\right)\cos\omega t - \frac{2\dot{y}_s(0)}{\omega}\sin\omega t - 6y_s(0) - \frac{3\dot{x}_s(0)}{\omega} \tag{9b}$$

$$y_s(t) = -\left(\frac{2\dot{x}_s(0)}{\omega} + 3y_s(0)\right)\cos\omega t + \frac{\dot{y}_s(0)}{\omega}\sin\omega t + 4y_s(0) + \frac{2\dot{x}_s(0)}{\omega} \tag{9c}$$

$$\frac{\dot{y}_s(t)}{\omega} = \left(\frac{2\dot{x}_s(0)}{\omega} + 3y_s(0)\right)\sin\omega t + \frac{\dot{y}_s(0)}{\omega}\cos\omega t \tag{9d}$$

where $\dot{x}_s(0)$, $\dot{y}_s(0)$, $x_s(0)$, and $y_s(0)$ refer to conditions at specified positions along the ballistic trajectory. These equations differ in sign from those in reference 3 because of the clockwise rotation of the moving-axis system used in this investigation. With the aid of equations (9b) and (9c), equation (8) can be written as

$$A(t)\frac{\dot{x}_s(0)}{\omega} + B(t)y_s(0) + C(t)\frac{\dot{y}_s(0)}{\omega} = D(t) \tag{10}$$

where $A(t)$, $B(t)$, $C(t)$, and $D(t)$ are defined as follows:

$$A(t) = (3 - 4\cos\omega t) + \frac{\omega_{ls}}{\omega}(2 - 2\cos\omega t)$$

$$B(t) = (6 - 6 \cos \omega t) + \frac{\omega_{ls}}{\omega} (4 - 3 \cos \omega t)$$

$$C(t) = \left(2 + \frac{\omega_{ls}}{\omega}\right) \sin \omega t$$

$$D(t) = r_o - \frac{\omega_{ls}}{\omega} h_o$$

An equation that expresses the maximum displacement in the y_s-direction can be obtained from equations (9c) and (9d). This condition implies $\dot{y}_s(t) = 0$ and from equation (9d) the following equation is obtained

$$\omega t = \tan^{-1}\left(\frac{\frac{-\dot{y}_s(0)}{\omega}}{\frac{2\dot{x}_s(0)}{\omega} + 3y_s(0)}\right) \tag{11}$$

The substitution of equation (11) for ωt into equation (9c) results in the following equation for the maximum displacement in the negative $y_s(t)$ direction denoted by $\left(y_s\right)_p$

$$\left(y_s\right)_p = -\left(\frac{2\dot{x}_s(0)}{\omega} + 3y_s(0)\right) \cos \left[\tan^{-1}\left(\frac{\frac{-\dot{y}_s(0)}{\omega}}{\frac{2\dot{x}_s(0)}{\omega} + 3y_s(0)}\right)\right]$$

$$+ \frac{\dot{y}_s(0)}{\omega} \sin \left[\tan^{-1}\left(\frac{\frac{-\dot{y}_s(0)}{\omega}}{\frac{2\dot{x}_s(0)}{\omega} + 3y_s(0)}\right)\right] + 4y_s(0) + \frac{2\dot{x}_s(0)}{\omega} \tag{12}$$

The pericynthion of the orbit is

$$h_p = \left(y_s\right)_p + h_o \tag{13}$$

Equations (10) to (13) are used to predict orbit pericynthion based on values of angular velocity of the line of sight with respect to a lunar surface feature.

To determine the three variables $\dot{x}_s(0)$, $\dot{y}_s(0)$, and $y_s(0)$ in equation (10) requires that three consecutive values of ω_{ls} and associated times t in orbit be available. The magnitude of ω_{ls} used in the derived equations was calculated from the expression $\omega_{ls} = r\dot{\theta}/h$ (for $\phi = 0$) at selected times along the known elliptical transfer orbits. The times were measured from the apocynthion of the orbits. The coefficients A, B, C, and D were evaluated, after which standard procedures for solving simultaneous equations were used to obtain the relative velocity and displacement components $\dot{x}_s(0)$, $\dot{y}_s(0)$, and $y_s(0)$. These values were assumed to be the conditions at the time of the first ω_{ls} measurement and were used to predict pericynthion altitude h_p from equation (13) with the aid of equations (11) and (12).

RESULTS AND DISCUSSION

Three ballistic trajectories were selected for use in the evaluation of the equations derived herein. Each had an apocynthion of 148 160 meters and had pericynthion altitudes of 27 611 meters, 10 862 meters, and -186 meters. Values of ω_{ls} were calculated along each of the trajectories (fig. 3) and these were used in subsequent computations. Since a number of approximations and assumptions were made in the derivation of the equations, it was realized that there would be errors involved in the predicted pericynthion altitudes. During this study the effects of the following variables were examined: time of assumed ω_{ls} measurements, reference orbit altitude, and error in estimated initial conditions.

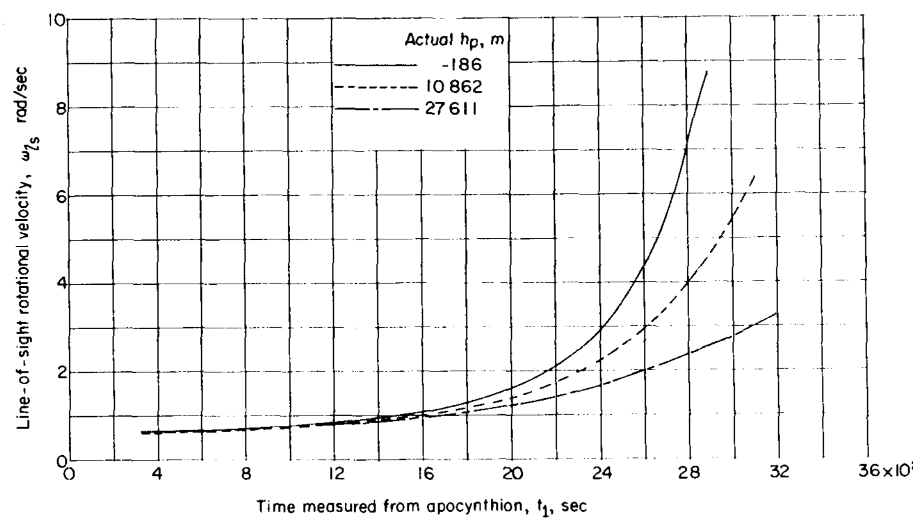

Figure 3.- Variation of ω_{ls} for three selected descent ballistic trajectories. $\Phi = 0$.

Effect of Assumed Time of ω_{ls} Measurements

The reference circular selenocentric orbit, which contains the origin of the moving-axis system, passes through the apocynthion of the transfer orbit. Time was assumed to be measured from apocynthion. The computed initial conditions corresponded to the conditions at various times from apocynthion. As mentioned previously, these initial values were assumed to be the conditions at the first ω_{ls} measurement. The predicted pericynthion altitudes for the three reference descent orbits are shown in figure 4 plotted against time measured from apocynthion to the first ω_{ls} value. The specific times used for the assumed ω_{ls} measurements are given in table I. These times were chosen arbitrarily to extend from apocynthion to near pericynthion (about one-half the orbital period). A study of figure 4 shows that the trends are the same for all three orbits, and generally indicate pericynthion altitudes lower than the reference-orbit pericynthions. However, these results indicate an improved prediction as the time for measurement is delayed.

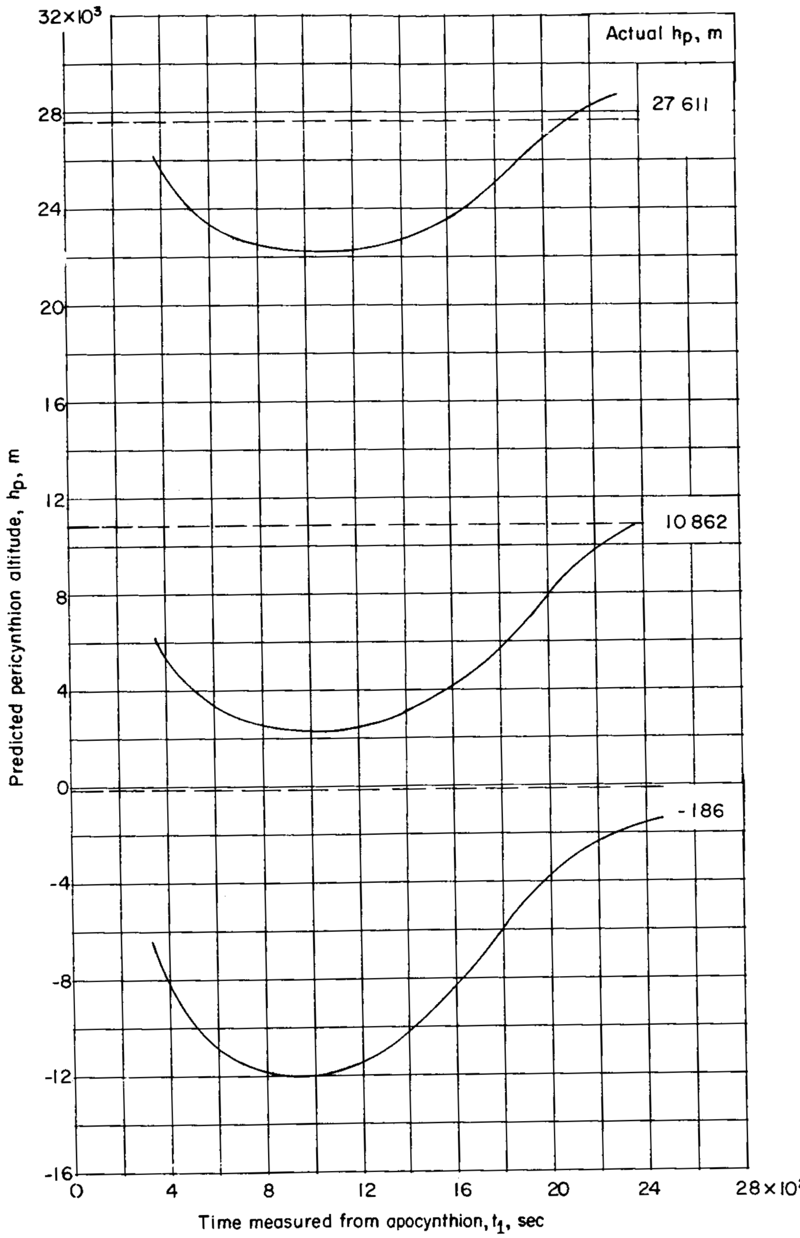

Figure 4.- Predicted pericynthion altitude plotted against time of first ω_{ls} value. Reference circular orbit altitude of 148 160 meters.

TABLE I.- PREDICTED h_p CALCULATED FROM THREE VALUES OF ω_{ls} AND THE ERROR Δh_p AS A FUNCTION OF VARIOUS ORBITAL TIMES

[Reference circular orbit altitude of 148 160 meters]

h_p, reference, m	t, seconds, measured from apocynthion			h_p, predicted, m	Δh_p, m
	t_1	t_2	t_3		
27611	383	701	1274	26136	-1475
	701	1108	1718	22752	-4859
	1108	1718	2421	22440	-5171
	1575	1859	2296	22835	-4776
	1859	2296	2655	25908	-1703
	2145	2533	3193	28477	866
	2315	2655	3193	28680	1069
10862	361	863	1459	6079	-4783
	658	1186	1711	3028	-7834
	863	1186	1586	2245	-8617
	1186	1711	2551	3348	-7514
	1459	1711	2182	2056	-8806
	1711	2098	2452	5112	-5750
	2082	2452	2921	9444	-1418
	2358	2659	3106	10893	31
-186	345	826	1391	-6488	-6302
	629	1134	1854	-11301	-11115
	989	1391	1854	-12520	-12334
	1134	1854	2465	-9654	-9468
	1511	1968	2377	-9348	-9162
	1627	2058	2465	-8099	-7913
	1854	2213	2658	-5508	-5322
	1982	2465	2898	-3049	-2863
	2465	2658	2898	-1428	-1242

Some calculations were also made for a pericynthion altitude of 10 862 meters in which the time interval between ω_{ls} measurements were approximately constant. The results of these calculations are presented in figure 5, as predicted h_p values plotted against time of the first ω_{ls} measurement. Three approximately constant time intervals of 200, 600, and 1000 seconds are shown in figure 5. For purposes of comparison, the results for the arbitrary intervals (nonconstant) are also presented. The nonconstant time intervals were generally in the vicinity of 200 to 600 seconds. A study of this figure shows that predicted h_p values closer to the true value of h_p were obtained by lengthening the time interval between assumed ω_{ls} measurements. (Compare results for 200, 600, and 1000 seconds.) It should be noted that this effect occurred primarily at the larger values of delay time from apocynthion. This trend suggests that predicted h_p values in the neighborhood of the true values can be obtained by a proper selection of ω_{ls} measurement as a function of delay time from apocynthion. However, it should be pointed out that the total time necessary to obtain the necessary three ω_{ls} measurements for a

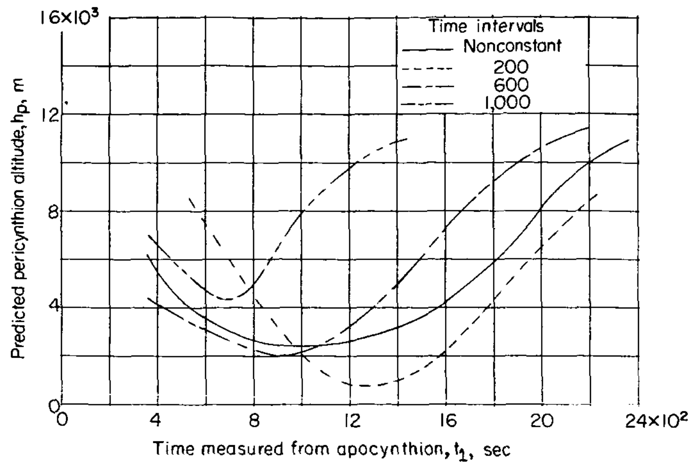

Figure 5.- Variation of predicted pericynthion altitude with time plotted at first ω_{ls} value for several constant time intervals between assumed measurements. Reference selenocentric orbit, 148 160 meters.

reasonably accurate prediction required that the last measured value occur so close to the time of pericynthion that sufficient time for corrective measures may not be available in the event that a dangerously low altitude was predicted.

The error in predicting pericynthion altitude, based on the results in table I, is shown in figure 6. This figure presents Δh_p plotted against time measured from apocynthion to the first ω_{ls} value. The error in predicted pericynthion altitudes varies inversely with actual pericynthion altitude. This variation appeared reasonable since the linearized rendezvous equations have an inherent assumption that gravity varies linearly from the reference orbit altitude. This result seems to indicate that a reference altitude closer to the average orbit altitude would be better than one at either extreme of the actual orbit. The magnitude of the error can be reduced somewhat by lengthening the intervals between ω_{ls} measurements. This result can be inferred, for 10 862-meter pericynthion orbit, from a comparison of the results in figures 5 and 6.

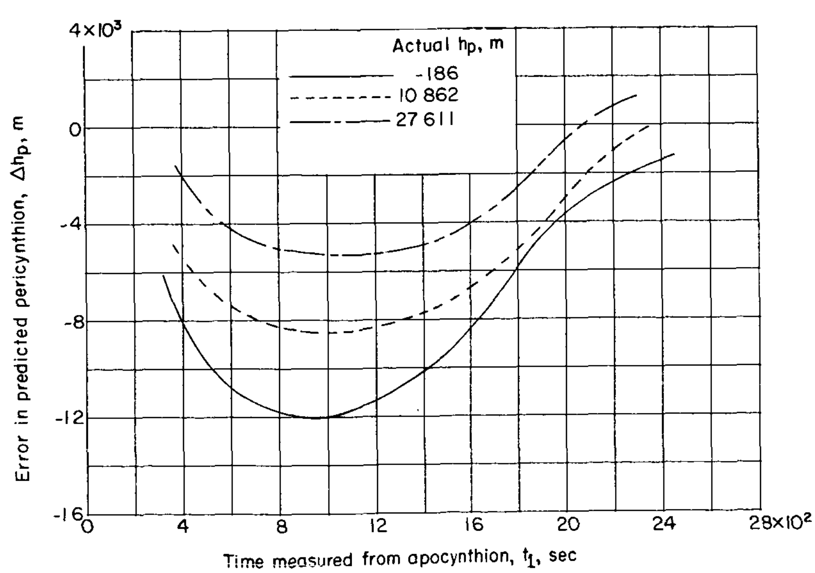

Figure 6.- Error in predicted pericynthion altitude plotted against time of first ω_{ls} value. Reference circular orbit altitude of 148 160 meters.

Effect of Reference Orbit Altitude

A series of computations were made with the origin of the moving-axis system in a circular orbit at an altitude of 74 080 meters, that is, one-half of the maximum orbit altitude. It was further assumed that the landing vehicle initiated its descent maneuver from the maximum orbit altitude of 148 160 meters. The results are shown in figure 7, which shows the predicted pericynthion altitudes plotted against time measured from apocynthion to the first ω_{ls} value.

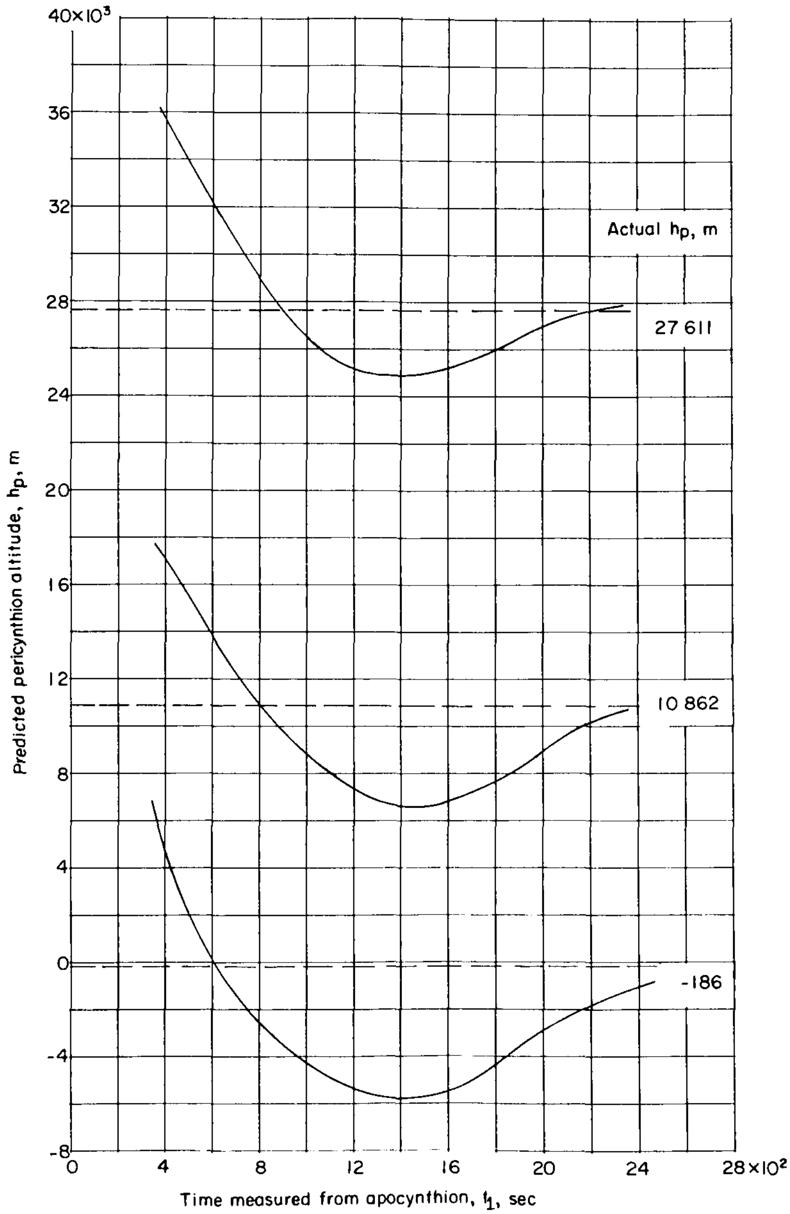

Figure 7.- Predicted pericynthion altitude plotted against time of first ω_{ls} value. Reference circular orbit altitude of 74 080 meters.

Table II indicates the times at which the ω_{ls} values were obtained. A comparison of figure 7 with figure 4 shows that decreasing the altitude of the reference selenocentric orbit did not appreciably affect the trends of the variation of h_p with time of measurement; it did, however, shift the entire pattern upward toward higher values of h_p. Thus, the predicted values of h_p were higher than the true values at small delay times and somewhat closer to the actual values at the larger delay times than the results for the higher reference orbit.

Results for calculations made with approximately constant time intervals between readings are presented in figure 8 for a pericynthion altitude of 10 860 meters. This figure presents predicted h_p values plotted against time measured from apocynthion for constant time intervals of about 200, 600, and 1000 seconds. Also included in this figure are the results for nonconstant time intervals. A comparison of figure 8 with figure 5

TABLE II.- PREDICTED h_p CALCULATED FROM THREE VALUES OF ω_{ls} AND THE ERROR Δh_p AS A FUNCTION OF VARIOUS ORBITAL TIMES

[Reference circular orbit altitude of 74 080 meters]

h_p, reference, m	t, seconds, measured from apocynthion			h_p, predicted, m	Δh_p, m
	t_1	t_2	t_3		
	383	701	1274	36170	8559
	701	1108	1718	30280	2669
	1108	1718	2421	25536	-2075
27611	1575	1859	2296	25145	-2466
	1859	2296	2655	26224	-1387
	2145	2533	3193	27745	134
	2315	2655	3193	27868	257
	361	863	1459	17671	6809
	658	1186	1711	12483	1621
	863	1186	1586	11748	886
10862	1186	1711	2551	7078	-3784
	1459	1711	2182	6543	-4319
	1711	2098	2452	7264	-3598
	2082	2452	2921	9690	-1172
	2358	2659	3106	10710	-152
	345	826	1391	6968	7154
	629	1134	1854	-754	-568
	989	1391	1854	-3631	-3445
-186	1134	1854	2465	-5159	-4973
	1511	1968	2377	-5625	-5439
	1627	2058	2465	-5147	-4961
	1854	2213	2658	-3813	-3627
	1982	2465	2898	-2291	-2105
	2465	2658	2898	-1132	-946

again shows the upward shift and the similarity of the trends of variation with time of measurement. These characteristics have been discussed previously for figure 5. The data of figure 9 show the error in predicted h_p altitude as a function of the time of the first ω_{ls} measurement. The effects of decreasing the orbit altitude to 74 080 meters (which were pointed out previously) are shown in this figure. As pointed out earlier, some reduction in the magnitude of the error can be obtained by lengthening the time interval between ω_{ls} measurements. (Compare results in figs. 8 and 9 for the 10 862-meter pericynthion.)

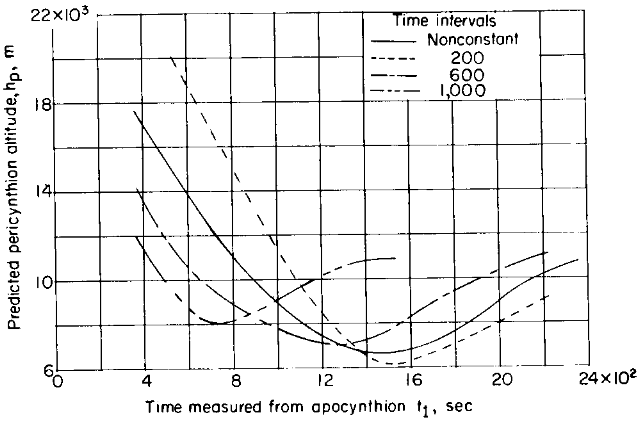

Figure 8.- Variation of predicted pericynthion altitude with time plotted at first ω_{ls} value for several constant time intervals between assumed measurements. Reference selenocentric orbit, 74 084 meters.

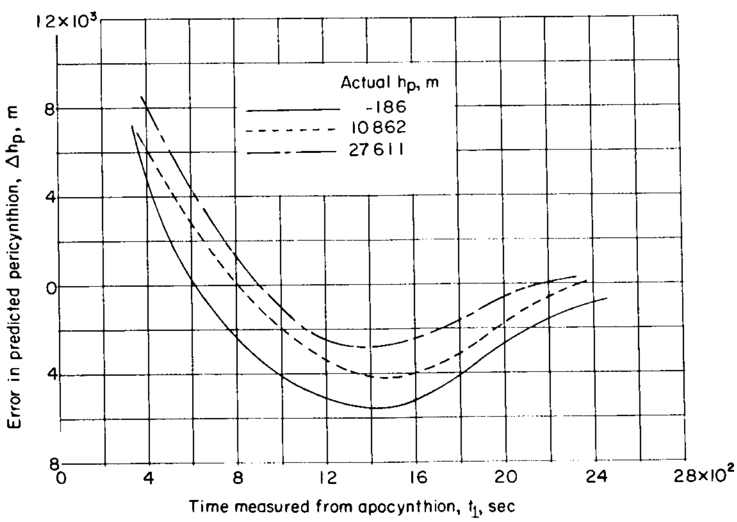

Figure 9.- Error in predicted pericynthion altitude plotted against time of first ω_{ls} value. Reference circular orbit altitude of 74 080 meters.

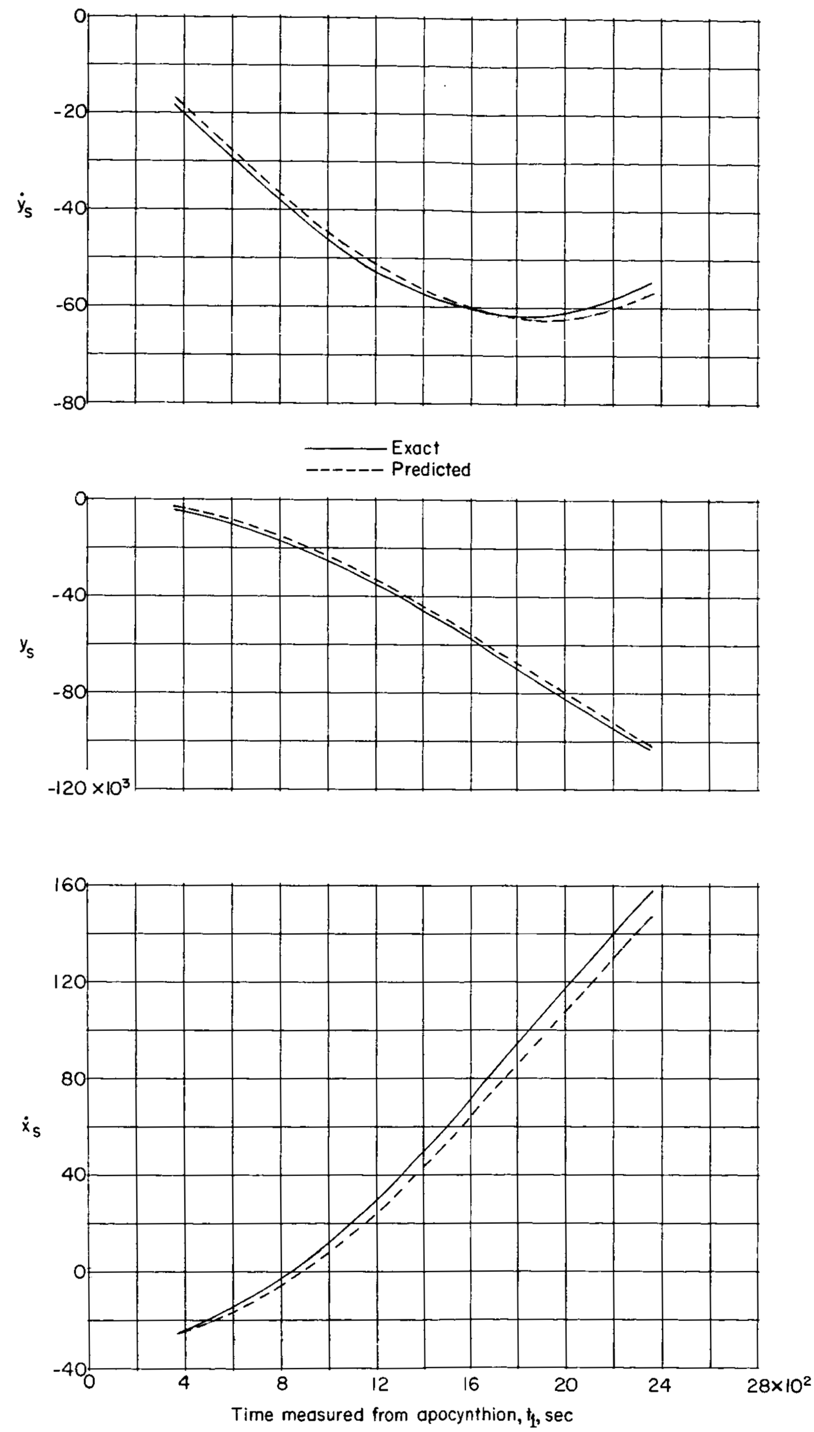

Figure 10.- Comparison of estimated and exact initial conditions plotted against time of first ω_{ls} value for orbit with 10 862-meter pericynthion.

Sources of Errors in Predicted Pericynthions

Errors in predicted pericynthion were very sizable in some cases. There appeared to be two possible major sources of error: the estimated initial conditions, and the use of the approximate equations for estimating pericynthion altitude.

Figure 10 compares the exact and the estimated initial conditions (based on calculated ω_{ls} values) at the time of the first ω_{ls} reading. The differences in these exact and estimated values for the initial conditions diverge as t_1 increases, and suggest the increased importance of second-order terms neglected in the derivation of equation (10). The divergence in estimated and exact initial values varies regularly and, therefore, would not account for the type of Δh_p variation shown in figures 6 and 9.

At this point the exact initial conditions (values obtained from exact orbit equations) were used with the pericynthion prediction equations (that is, equations (11), (12), and (13)), and results are shown in figure 11. This figure shows a comparison of estimated h_p obtained by using these exact values and by using estimated initial conditions based on ω_{ls} measurements. It is apparent that use of the exact initial conditions in the approximate equations generally does not improve the estimated pericynthion prediction. To some extent the use of exact initial conditions made matters worse in that there is no longer a convergence toward the proper value as the time for ω_{ls} measurements is

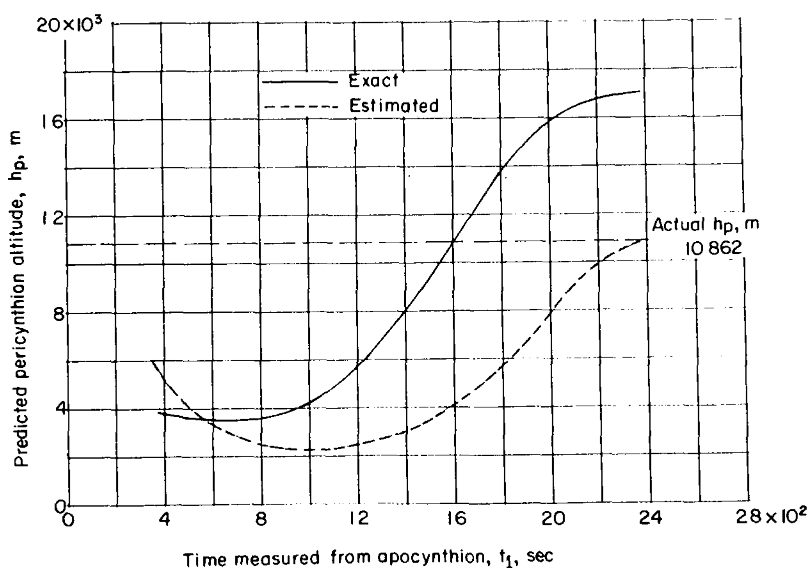

Figure 11.- Comparison of pericynthion altitudes calculated from exact and estimated initial conditions for orbit with 10 862-meter pericynthion. Linearized rendezvous equations were used for exact calculations. Reference circular orbit altitude was 148 160 meters.

delayed; the value to which the predictions appear to converge overestimates pericynthion altitude. These trends suggest that perhaps better results could be obtained with this procedure $\left(\omega_{ls}\right.$ measurement$\left.\right)$ if an improved set of linearized equations could be developed.

CONCLUDING REMARKS

An investigation was made to determine the feasibility of using simplified equations to predict orbit pericynthion. It was assumed that the angular rate of the line of sight with respect to a prominent lunar surface feature was available for positions along selenocentric orbits. The equations used were derived in terms of this variable by utilizing the linearized equations of relative motion of orbiting bodies and certain parameters of a circular selenocentric orbit. The procedure used for the evaluation of these equations was to calculate pericynthion altitudes of known reference orbits and to compare the estimated values with the actual values.

The results of the computations indicate that

(1) The pericynthion altitude predicted by the approximate equations generally is not accurate.

(2) The predicted pericynthion altitude is very sensitive to the reference orbit altitude and to the times (location in the transfer orbit) at which measurements of the rotation of the line of sight are made, and to the length of time between the measurements of the angular rate of line of sight.

Langley Research Center,
National Aeronautics and Space Administration,
Langley Station, Hampton, Va., August 31, 1967,
125-17-05-01-23.

REFERENCES

1. Gersten, Robert H.; and Schwarzbein, Z. E.: Self-Contained Orbit Determination Techniques. [Paper] No. 63-431, Am. Inst. Aeron. Astronaut., Aug. 1963.

2. Reid, Richard: A Simplified Technique for Determining Deviation in the Lunar Transfer Orbit Ephemeris. NASA TN D-1837, 1964.

3. Eggleston, John M.; and Beck, Harold D.: A Study of the Positions and Velocities of a Space Station and a Ferry Vehicle During Rendezvous and Return. NASA TR R-87, 1961.

NASA-Langley, 1968 —— 30 L-5296